



CHORUS

This is the accepted manuscript made available via CHORUS. The article has been published as:

Elasticity of Nuclear Pasta

M. E. Caplan, A. S. Schneider, and C. J. Horowitz

Phys. Rev. Lett. **121**, 132701 — Published 24 September 2018

DOI: [10.1103/PhysRevLett.121.132701](https://doi.org/10.1103/PhysRevLett.121.132701)

The Elasticity of Nuclear Pasta

M. E. Caplan,^{1,*} A. S. Schneider,² and C. J. Horowitz^{3,†}

¹*McGill Space Institute, McGill University, 3600 Rue University, Montreal, QC Canada H3A 2T8*

²*TAPIR, Walter Burke Institute for Theoretical Physics,*

California Institute of Technology, Pasadena, CA 91125, USA

³*Nuclear Theory Center, Indiana University, Bloomington, IN 47401, USA*

(Dated: August 28, 2018)

The elastic properties of neutron star crusts are relevant for a variety of currently observable or near-future electromagnetic and gravitational wave phenomena. These phenomena may depend on the elastic properties of nuclear pasta found in the inner crust. We present large scale classical molecular dynamics simulations where we deform nuclear pasta. We simulate idealized samples of nuclear pasta and describe their breaking mechanism. We also deform nuclear pasta that is arranged into many domains, similar to what is known for the ions in neutron star crusts. Our results show that nuclear pasta may be the strongest known material, perhaps with a shear modulus of 10^{30} ergs/cm³ and breaking strain greater than 0.1.

Introduction. The breaking strain of materials in neutron star (NS) crusts are relevant for a variety of electromagnetic and gravitational wave phenomena. Crust breaking may occur in magnetar outbursts [1], resonant crust shattering in NS mergers [2], and in the starquake model for pulsar glitches [3, 4]. Likewise, the shear modulus of crust matter may affect the oscillation frequency of magnetar flares [5], the damping of r-modes [6], and determine the height and lifetime of mountains on a NS [4, 7].

The crust comprises the outermost kilometer of the NS, where the density goes from near vacuum at the surface to nuclear density (10^{14} g/cm³) at the base. The outer crust is a bcc lattice of nuclei embedded in a gas of degenerate electrons, which becomes increasingly neutron rich with depth [8, 9]. At the base of the inner crust the separation between nuclei becomes comparable to nuclei radii and nucleons rearrange themselves into complex shapes known as nuclear pasta [10, 11]. The pasta layer may be 100-250 m thick, but due to its high density may contain half the total mass of the crust or more [12]. It is therefore essential to understand the elastic properties of this material, as it may play an important role in crust breaking and be the dominant source of continuous gravitational waves that aLIGO is now searching for [13].

Past works have studied elastic properties (breaking strain and shear modulus) of the ion crust with both molecular dynamics (MD) and analytic methods [4, 8, 9, 14–16]. The ion crust is understood to be a polycrystalline bcc lattice, *i.e.*, composed of microscopic domains with different orientations. Thus, over sufficiently large length scales the crust is treated as an isotropic material whose properties are found by angle averaging bcc lattice properties [16]. MD simulations suggest that domains lead to an effective angle-averaged shear modulus [4, 15] and that high pressure prevents voids from forming and fractures from propagating, thus, leading to a relatively high breaking strain $\epsilon \approx 0.1$ [15].

Presently, the pasta is less well understood. Unlike

the ion lattice pasta is not a crystal but, rather, a liquid crystal. Pethick & Potekhin, Ref. [17], were the first to study the elasticity of nuclear pasta. They considered the energy of deformation E_d of parallel pasta plates to be

$$E_d = \frac{B}{2} \left[\frac{\partial u}{\partial z} - \frac{1}{2} (\nabla_{\perp} u)^2 \right]^2 + \frac{K_1}{2} (\nabla_{\perp}^2 u)^2, \quad (1)$$

where B and K_1 are elastic constants and u the displacement between plates along the z axis (plate normal) [17]. The first term is the energy due to the separation of the plates. The $(\nabla_{\perp} u)^2$ term is due to rotational invariance, as out-of-plane shear is rotationally equivalent to changing the plate spacing. The last term is due to splay deformations (plate curvature).

These analytic techniques are difficult to apply to asymmetric pasta or pasta lacking long range order. Even short range disorder such as helicoidal defects (filaments connecting the plates) may support shear stresses between plates. These may be difficult to predict analytically, but can be studied using MD simulations. The same is true for the effect of domains and their boundaries in nuclear pasta on crust elasticity.

Watanabe et al. compare the typical thermal energy to the energy of deformation of nuclear pasta and find that pasta deforms on length scales of order ten times its spacing [18]. This result is supported by quantum mechanical simulations that suggest that the pasta, like the ion crust, does not have a uniform orientation across the star [19]. Rather, nuclear pasta should be composed of many microscopic domains with distinct orientations. Thus, calculations of the elastic properties of the crust should consider ‘polycrystalline’ nuclear pasta with many domains. Currently, such studies are limited to MD simulations since those can simulate large volumes with multiple domains [20] while quantum mechanical simulations are limited to a few thousand nucleons [21].

In this Letter we discuss MD simulations (1) deforming nuclear pasta plates, to understand the breaking of

its elementary units, and (2) deforming a large nuclear pasta system with multiple domains, to understand angle averaged elastic properties of nuclear pasta.

Simulations. Our simulations are performed using the Indiana University Molecular Dynamics code v6.3.1 (IUMD), which has been used extensively to simulate nuclear pasta [9, 22, 23]. In our model, two nucleons i and j separated by a distance r interact via the two-body potential

$$V_{ij}(r) = ae^{-r^2/\Lambda} + [b \pm c]e^{-r^2/2\Lambda} + \frac{e_i e_j}{r} e^{-r/\lambda}. \quad (2)$$

The parameters a , b , c , and Λ are chosen to reproduce the binding energy of nuclei, pure neutron matter, and symmetric nuclear matter while λ is the Thomas-Fermi screening length, fixed at 10 fm for simplicity [22]. The $b+c$ ($b-c$) term sets a weak (strong) attraction between like (alike) nucleons. The electric charges e_i and e_j produce long range Coulomb repulsion between protons. All systems are simulated at temperature $T = 1$ MeV and nucleon number density $n = 0.05 \text{ fm}^{-3}$.

Our first simulations contain 102 400 nucleons at a proton fraction $Y_P = 0.4$, where pasta is expected to form ‘lasagna’ plates [9, 23]. This proton fraction is higher than expected in the inner crust, but is where our model forms pasta; at more realistic proton fractions the classical model produces a gas of protons and neutrons [24].

We initialize our simulation with a cubic volume (side length l_0) with periodic boundary conditions and apply volume preserving deformations. During a simulation, we apply constant extensional strain along axis r and contract along the other two, s and t , by adjusting the box boundary position slightly after each MD timestep, *i.e.*,

$$l_r(t) = l_0(1 + \dot{\epsilon}t) \quad \text{and} \quad l_s(t) = l_t(t) = \frac{l_0}{\sqrt{1 + \dot{\epsilon}t}}. \quad (3)$$

where $\dot{\epsilon}$ is the strain rate and r , s , and t are permutations of x , y , and z . Nucleons may have an arbitrary initial arrangement and respond dynamically to the changing simulation volume. The induced stresses are calculated using

$$\sigma_{\alpha\beta} = \frac{1}{V} \sum_i \left[-m u_{\alpha}^{(i)} u_{\beta}^{(j)} + \sum_{i < j} (x_{\beta}^{(i)} - x_{\alpha}^{(i)}) f_{\beta}^{(ij)} \right]. \quad (4)$$

Above, V is the simulation volume, m the nucleon mass, $x_{\alpha}^{(i)}$ ($u_{\alpha}^{(i)}$) the α component of the position (velocity) of nucleon i and $f_{\beta}^{(ij)}$ the β component of the force nucleon i exerts on nucleon j . Repeated (mixed) lower indices denote tensile (shear) stress.

Although these are purely tensile strains, they can be transformed into shear strains by having the pasta structures oriented at an angle with respect to the simulation boundaries. Furthermore, nuclear pasta is not

necessarily linearly elastic. Lasagna, for example, has transverse isotropy implying five independent elastic constants. Misalignment of the pasta structures with respect to the boundary and their time evolution makes it difficult to isolate these constants for all but the simplest cases. For most simulations, we observe a rotated stress tensor which mixes all σ terms.

We strain at rates $\dot{\epsilon} = 1 \times 10^{-7}$ and 2×10^{-7} c/fm until a final strain $\epsilon_r = 1$ along the axis of extension is achieved. This results in a compressional strain of $\epsilon_s = \epsilon_t = 1/\sqrt{2} \approx 0.29$ in the other two axes. This choice of strain rate does not affect our results. Although these deformations are much greater than those realized in astrophysical systems, they allow us to observe the breaking behavior of nuclear pasta.

First we deform ‘perfect’ plates which are aligned with the xy plane of the simulation volume [26]. In the first case, Fig. 1a, we strain along the z direction, pulling the plates apart, while contracting along the plate plane. For $\epsilon_z > 0.05$ the plates start to buckle to maintain their initial spacing. Tensile stress along z remains constant from then on, while the stress in the plates decrease as the plates buckle. The plates deform continuously without breaking up till a strain $\epsilon_z = 1$. As expected, no significant shear stresses are observed in this run.

In the second case, Fig. 1b, we strain along the x axis, pulling along the plates and allowing their spacing to contract. Tensile stress along the z direction grows as Coulomb pressure between plates increases. Meanwhile, in-plane stress decreases with the thinning of the plates. At $\epsilon_x \approx 0.3$ ($\epsilon_z \approx 0.13$), the plates break and the stresses abruptly change. The stresses reset and the process continues until another breaking event occurs at $\epsilon_x \approx 0.8$. To our knowledge, this breaking mechanism has not been described elsewhere in the literature so we describe it here in detail. We observe that (1) for small strains the spacing between plates decreases while the plates themselves become thinner. (2) Once the plates are thin enough, thermal fluctuations nucleate holes in them. (3) By displacing nucleons in the plate the holes relieves the Coulomb pressure between adjacent plates. (4) Adjacent plates become convex in the region of the holes. This partially fills the space vacated by the holes and allows the plates to increase their spacing locally, further reducing the system’s pressure. (5) Convex lobes from the adjacent plates connect near the hole, forming short helicoidal bridges that connects adjacent plates. This allows connected plates to exchange nucleons. This process occurs in several locations simultaneously, allowing the plates to thicken and increase their interspacing locally. The bridges then drift through the plates until they are aligned, as seen in Fig. 1b, suggesting there is long range attraction between them as predicted by Guven *et al.* [27]. Once the plates reach their ideal thickness the bridges thin and disconnect, resulting in planar lasagna but with one fewer plate spanning the simulation volume.

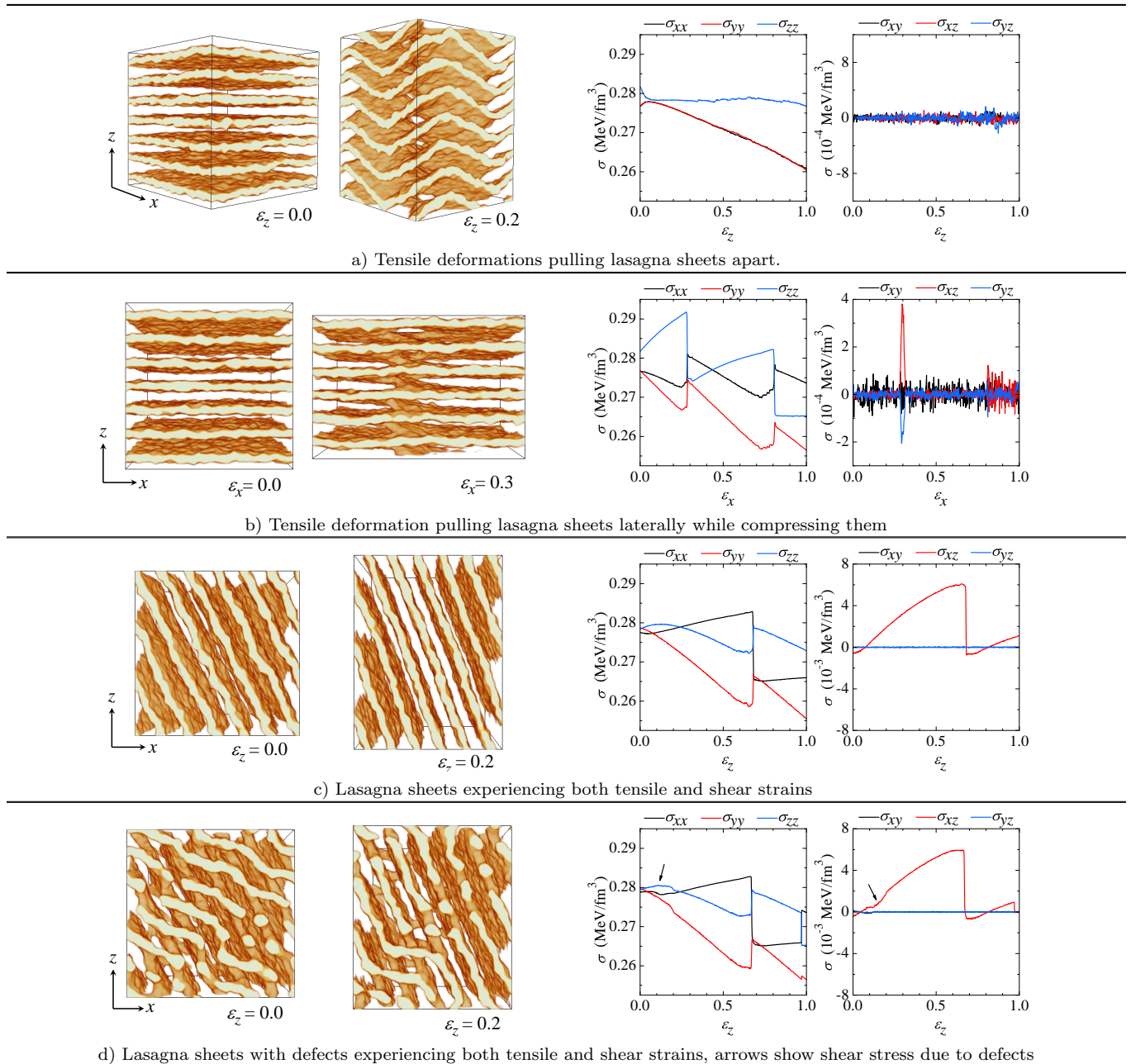


FIG. 1. Simulations deforming idealized nuclear pasta. Left to right, (1) initial configuration of the pasta, (2) deformed pasta at some later time, (3) tensile stresses vs. extensional strain, and (4) shear stresses vs. extensional strain. Strain $\epsilon_r = l_r(t) - l_0$, see Eq. (4), is proportional to time. Animations available in SM1-4 [25].

During the first breaking event we observe that the shear stresses in the xz and yz planes are briefly nonzero, suggesting that bridges can support shear stresses between plates.

While the helicoidal bridges were short lived in this simulation, past work has identified stable configurations where filaments connecting plates are long lived [28]. These may support shear stresses between plates and, perhaps, even act as grain boundaries between domains where pasta plates have different orientations.

We also consider simulations of lasagna plates which are misaligned with the sides of the box allowing us to induce shear stresses in the material. In Fig. 1c the pasta plates are rotated in the xz plane, while in Fig. 1d plates are similarly oriented but connected by stable long lived filaments. Both systems have similar energy, suggesting that pasta has multiple available phases to it [19].

The plates in Fig. 1c are free to adjust their inclination in response to the applied strain. They first break near $\epsilon_z \approx 0.68$, implying that pasta breaks less easily

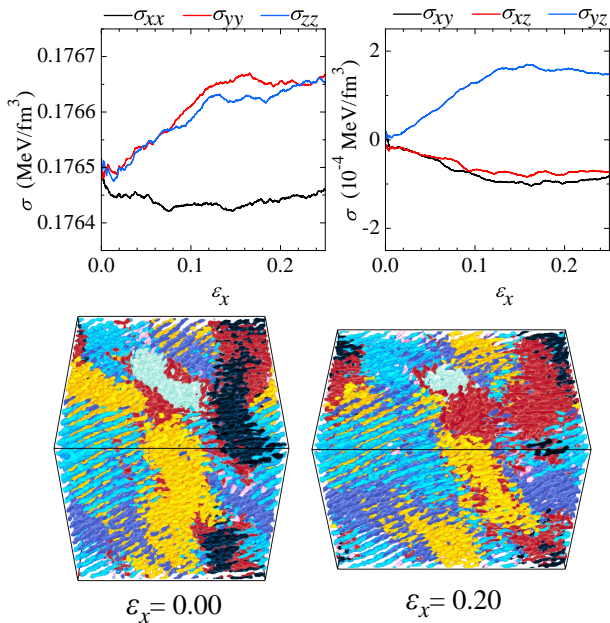


FIG. 2. Multidomain simulation of strained nuclear pasta. (Top) Tensile, left, and shear stresses, right. (Bottom) Evolution of domains, identified by color, from no strain ($\epsilon_x = 0.0$), left, to $\epsilon_x = 0.2$, right. Animations in SM5,6 [25].

when the plates can adjust their inclination. The shear stress in the xz plane grows approximately linearly until the break, transforming a tensile stress into a shear stress as expected. However, these shear stresses can be eliminated by applying a rotation matrix to the stress tensor whose angle is taken from the inclination of the plates, approximately recovering the stresses seen in Fig. 1b, as expected. This directly confirms that disconnected plates have near zero shear modulus between plates, as claimed by Pethick & Potekhin [17].

In the run with inclined plates connected by helicoidal defects, Fig. 1d, the tensile deformation of the boundary again produces a shear deformation of the plates in the xz plane. However, the filaments initially resist this shear. The filaments break near $\epsilon_y \approx 0.2$, at which point the evolution proceeds identically to the case discussed in Fig. 1c.

The difference in σ_{xz} at small strains between Fig. 1c and Fig. 1d cannot be eliminated by applying a rotation and is a clear indication of a shear modulus produced by the filaments. Their difference gives a maximum shear stress of 3×10^{-4} MeV/fm³; estimating the shear strain to be 0.1 gives us a shear modulus of 5×10^{30} erg/cm³. The rotation of the plates partially transforms the shear stress into a tensile stress at small strains, so this shear modulus may be a factor of two larger.

With the elastic response of individual domains of nuclear pasta understood, we now consider a larger simulation with many domains. This simulation contains 3 276 800 nucleons at proton fraction $Y_P = 0.3$. These

parameters are known to produce parallel plates with a hexagonal arrangement of holes, the ‘waffle’ phase [24]. This proton fraction was chosen for two reasons. First, the simulation is less computationally expensive and allows us to evolve a larger number of particles. Second, the filamentary structure of the waffles allow us to study how domains and asymmetry affect pasta elasticity.

This is the largest simulation of nuclear pasta yet and its preparation is discussed in detail in Ref. [20]. Briefly, we evolved a random initial state for over 15,250,000 MD timesteps and the system formed seven differently oriented domains, see Fig. 2. The plates are misaligned at domain boundaries, but topologically connected by filaments. The relative volume fractions of domains remained approximately constant during this initial evolution, suggesting the domains are long lived.

This simulation was strained at a rate $\dot{\epsilon}_x = 2 \times 10^{-7}$ c/fm until $\epsilon_x = 0.25$. The stresses are shown in Fig. 2. No breaking was observed. Shear and tensile stresses with components perpendicular to the strain direction x grow approximately linearly until $\epsilon_x \sim 0.12$ and then flatten out. Meanwhile, stresses with x components decrease slightly before flattening out. This is expected for a linear isotropic material which is misaligned with the strain axis. Another simulation was strained at $\dot{\epsilon}_x = 1 \times 10^{-6}$ c/fm until $\epsilon_x = 0.77$ and found similar results. While it is not possible to extract individual elastic constants from this simulation, the stresses grow comparably to our $Y_P = 40\%$ simulations, suggesting they may be similar.

In Fig. 2 we show our simulation for two different strains, $\epsilon_x = 0.0$ and 0.2. At their boundaries, domains are connected by filaments similar to the helicoidal defects considered above. When strained, domains move relative to each other and slide with limited resistance. At large strains, nucleons flow between adjacent domains at the boundaries, allowing domains to shrink or grow in response to the applied stress. This is a mechanism for plastic flow, possibly preventing catastrophic failures. If nuclear pasta forms domains, the inner crust may simply not break for realistic astrophysical strains.

Discussion. We find, using MD simulations, that the analytic model of Pethick & Potekhin describes well the qualitative elastic response of idealized lasagna plates to large deformations. Idealized nuclear pasta is strong in our model, possibly with a shear modulus as large as 10^{31} erg/cm³. This is comparable to the strength of the outer crust extrapolated to the high densities at the crust-core boundary, which may make nuclear pasta the strongest material in the known universe.

For comparison, a typical nucleus predicted at pasta densities by Haensel & Zdunik for an accreted crust is ⁸⁸Ti ($Z=22$) with free neutron fraction $X_n = 0.80$ [29]. Using the effective shear modulus of Horowitz & Hugtho $\mu_{eff} \sim 0.11nZ^2e^2/a$ (ion number density n , $a = [3/(4\pi n)]^{1/3}$) we find $\mu = 1.1 \times 10^{30}$ erg/cm³ [30]. We emphasize that the large shear modulus and break-

ing strain for our pasta simulations are model dependent. Our simulations use proton fractions much larger than those expected in the inner crust of NSs. A lower proton fraction likely reduces the shear modulus, perhaps to 10^{30} erg/cm³. This motivates further work on pasta elasticity, especially the role that superfluidity may play, which is beyond the scope of our simulations [31].

We explicitly describe the breaking mechanism, and find that the breaking strain of idealized nuclear pasta in the lasagna and waffle phases is large in our model, perhaps $\epsilon \approx 0.3$. This suggests that the ion crust breaks significantly earlier than the pasta. This may have consequences for crust breaking in a variety of systems, such as resonant shattering flares during neutron star mergers or magnetar outbursts.

Continuous gravitational wave searches [32] probe the ellipticity e (fractional difference in moments of inertia) of a rotating NS. The maximum e that an ion crust can support is $e_{max} \approx 4 \times 10^{-6}$ [15]. If μ and or ϵ are somewhat larger for pasta than for ions, this could lead to a larger e_{max} perhaps a few $\times 10^{-5}$ when nuclear pasta is included. As a result, LIGO observations of the Crab pulsar may now be sensitive to a maximally deformed crust that includes nuclear pasta [13].

Lastly, while this work describes the elastic response of some simple astromaterials, the variety of pasta shapes and their elastic responses may be difficult to describe with an analytic theory which motivates their continued study with molecular dynamics.

Acknowledgments. M.C. is a CITA National Fellow. A.S.S. is supported by the National Science Foundation under award No. AST-1333520 and CAREER PHY-1151197. C.J.H. supported in part by US Department of Energy grants DE-FG02-87ER40365 (Indiana University) and DE - SC0018083 (NUCLEI SciDAC-4 Collaboration). This research was supported in part by Lilly Endowment, Inc., through its support for the Indiana University Pervasive Technology Institute, and in part by the Indiana METACyt Initiative. The Indiana METACyt Initiative at IU was also supported in part by Lilly Endowment, Inc. We thank A. Cumming and A. Chugunov for conversation.

* matthew.caplan@mcgill.ca

† horowit@indiana.edu

- [1] C. Thompson and R. C. Duncan, *The Astrophysical Journal* **561**, 980 (2001).
- [2] D. Tsang, J. S. Read, T. Hinderer, A. L. Piro, and R. Bondarescu, *Phys. Rev. Lett.* **108**, 011102 (2012).
- [3] M. Ruderman, *Nature (London)* **223**, 597 (1969).
- [4] A. I. Chugunov and C. J. Horowitz, *Monthly Notices of the Royal Astronomical Society: Letters* **407**, L54 (2010).
- [5] T. E. Strohmayer and A. L. Watts, *The Astrophysical Journal* **653**, 593 (2006).
- [6] B. Haskell, N. Degenaar, and W. C. G. Ho, *Monthly Notices of the Royal Astronomical Society* **424**, 93 (2012).
- [7] S. Mahmoodifar and T. Strohmayer, *The Astrophysical Journal* **773**, 140 (2013).
- [8] N. Chamel and P. Haensel, *Living Reviews in Relativity* **11**, 10 (2008).
- [9] M. E. Caplan and C. J. Horowitz, *Rev. Mod. Phys.* **89**, 041002 (2017).
- [10] D. G. Ravenhall, C. J. Pethick, and J. R. Wilson, *Phys. Rev. Lett.* **50**, 2066 (1983).
- [11] M.-a. Hashimoto, H. Seki, and M. Yamada, *Progress of Theoretical Physics* **71**, 320 (1984).
- [12] W. G. Newton, *Nature Physics* **9**, 396 (2013).
- [13] B. P. Abbott *et al.* (LIGO Scientific Collaboration and Virgo Collaboration), *Phys. Rev. D* **96**, 122006 (2017).
- [14] M. E. Caplan, A. Cumming, D. K. Berry, C. J. Horowitz, and R. Mckinven, *The Astrophysical Journal* **860**, 148 (2018).
- [15] C. J. Horowitz and K. Kadau, *Phys. Rev. Lett.* **102**, 191102 (2009).
- [16] D. Kobyakov and C. J. Pethick, *Monthly Notices of the Royal Astronomical Society: Letters* **449**, L110 (2015).
- [17] C. Pethick and A. Potekhin, *Physics Letters B* **427**, 7 (1998).
- [18] G. Watanabe, K. Iida, and K. Sato, *Nuclear Physics A* **676**, 455 (2000).
- [19] W. Newton, (unpublished).
- [20] A. S. Schneider, M. E. Caplan, D. K. Berry, and C. J. Horowitz, (to be published).
- [21] F. J. Fattoyev, C. J. Horowitz, and B. Schuetrumpf, *Phys. Rev. C* **95**, 055804 (2017).
- [22] C. J. Horowitz, M. A. Pérez-García, and J. Piekarewicz, *Phys. Rev. C* **69**, 045804 (2004).
- [23] A. S. Schneider, C. J. Horowitz, J. Hughto, and D. K. Berry, *Phys. Rev. C* **88**, 065807 (2013).
- [24] A. S. Schneider, D. K. Berry, C. M. Briggs, M. E. Caplan, and C. J. Horowitz, *Phys. Rev. C* **90**, 055805 (2014).
- [25] Animations available at: www.physics.mcgill.ca/~mecaplan/pasta-elasticity/.
- [26] A. S. Schneider, D. K. Berry, M. E. Caplan, C. J. Horowitz, and Z. Lin, *Phys. Rev. C* **93**, 065806 (2016).
- [27] J. Guven, G. Huber, and D. M. Valencia, *Phys. Rev. Lett.* **113**, 188101 (2014).
- [28] C. J. Horowitz, D. K. Berry, C. M. Briggs, M. E. Caplan, A. Cumming, and A. S. Schneider, *Phys. Rev. Lett.* **114**, 031102 (2015).
- [29] P. Haensel and J. L. Zdunik, *Astronomy and Astrophysics* **229**, 117 (1990).
- [30] C. J. Horowitz and J. Hughto, *ArXiv e-prints* (2008), arXiv:0812.2650.
- [31] D. N. Kobyakov and C. J. Pethick, *ArXiv e-prints* (2018), arXiv:1803.06254 [nucl-th].
- [32] K. Riles, *Modern Physics Letters A* **32**, 1730035 (2017), <https://doi.org/10.1142/S021773231730035X>.